2016 IEEE Intelligent Vehicles Symposium (IV)
Gothenburg, Sweden, June 19-22, 2016

Modeling and Simulation of Rain for the Test of Automotive Sensor Systems

Sinan Hasirlioglu, Igor Doric, Christian Lauerer and Thomas Brandmeier
Center of Automotive Research on Integrated Safety Systems and Measurement Area (CARISSMA),
Technische Hochschule Ingolstadt, Germany, 85049
Email: {sinan.hasirlioglu, igor.doric, christian.lauerer, thomas.brandmeier}@thi.de

***Abstract*—This paper presents a new approach for the test of automotive sensor systems in rain. The approach is based on an indoor test method, which helps to save test kilometers and test effort. For the activation of safety systems detailed information about the vehicles environment is necessary. Laser scanners provide precise information about the environment and a high angular resolution in contrast to radar sensors [1]. The performance of laser scanners depends on their local environment, because of the attenuation of the ambient atmosphere, precipitation and on the reflectivity of objects. False measurements in the field of vehicle safety can result in severe injury or death, so high reliability is essential. For this purpose a theoretical model is developed in order to determine the sensor behavior. Subsequently, a rain simulator is constructed to validate the theoretical model. Furthermore the developed rain simulator is validated by comparison with real rain. Based on determined rain disturbances benchmark tests of different sensor systems and algorithm approaches can be performed.**

I. Introduction

The road safety model of Sweden has proven itself repeatedly as good practice. Its safety strategy aims to modify the environment in order to protect road users from unacceptable risk level. But road traffic injuries are still an important cause of death in Sweden. Road traffic crashes are responsible for deaths of every fifth child aged between 5 and 19 [2]. Due to this, integrated new safety systems has become a major topic of research in the automotive industry [3]. Integrated safety systems aim to completely avoid accidents or, in case of unavoidable collision, provide maximum protection to the vehicle occupants and also vulnerable road users (i.e. pedestrians). The detection of obstacles such as other vehicles, pedestrians and obstructions is an essential step in integrated safety and in operation of intelligent vehicles. Intelligent vehicles are sensing their environment using surround sensors and making decisions for autonomous operations. For automotive safety systems, laser scanners are becoming more important as an surround sensor, because of the high speed and accuracy. Disadvantage of laser scanners is the low weather resistance. Environmental factors such as rain or fog have significant impact on the detection of the environment. Especially in the area of safety, a false detection can have fatal consequences, for example, a false triggering of the airbag leads to the uncontrollability of the vehicle. Rain has be shown to be a major factor causing traffic accidents. When it rains occur up to 70% more accidents than normally occur [4]. Therefore, the automotive industry has to ensure very high reliability of safety systems. Field experiments have proven to be a good test method, however, these tests do not cover all environmental situations. Very much potential is seen in the field of indoor tests. In this field specific environmental influences can be tested in normal and very strong characteristics. A sufficiently good weather simulation can save high test effort and increase the reliability of sensor systems.

This paper is structured as follows. First the related work in the field of environmental influences on laser scanners is discussed. Based on this a new physical model, which describes the weather influences on laser scanners is presented. The distance between sensor and object is divided into individual layers, the effects that occur are then summarized. For the validation of the model a rain simulator is developed and constructed for deterministic indoor tests under different rain conditions. Additionally the rain simulator was validated by comparison with real rain.

II. Related Work

First ideas to describe the environmental influences on the lidar sensor can be found in [5], where Mie's theory is used for the calculation of extinction efficiency and the backscattering efficiency for a single rain drop. Rasshofer et al. [5] use a model according to Deirmendjian [6] for the distribution of rain droplets, which is based on a gamma distribution. It assumes, that light reflected by a single droplet is not reflected again, so no multiple reflections are considered. The experiments were carried out using a rain simulator, which simulates rain with an intensity of up to 27 mm/h. In [7] the calculation of atmospheric extinction coefficient were performed in FASCODE (Fast Atmospheric Signature Code) environment. This software performs accurate and fast calculations in various spectrums. In the project FRICTION environmental factors have been studied with an Ibeo laser sensor, which is capable of multi target detection. The acquisition of information about weather conditions is not a major requirement for this application, instead they demand robustness against adverse weather conditions [8]. Rain simulators are also used by meteorologists to study soil erosion. Hereby, the focus is on heavy rain with big rain drops [9]. However, for the test of surround sensors, it is important to reproduce a natural drop size distribution and rain intensity.

978-1-5090-1821-5/16/$31.00 ©2016 IEEE

III. MODELING

The idea of the new model is based on the abstraction to a layer model. The distance between sensor and object is divided into several layers. The thickness of one single layer depends on the sensor resolution. For example the ibeo LUX sensor detects obstacles in a maximum distance of 200 meters and can output its data with a distance resolution of 0.04 meters [10].

The physical effects of the interaction between light beam and rain drops are considered in steps. Within one layer the physical effect of rain are considered in sum. These are transmission, reflection and absorption. The transmitted light component passes into the next layer. The reflected light component reverses its direction and enters the previous layer or to the sensor. The absorbed energy is considered as loss of energy, and will not be further considered for the time of flight. The light path is divided into several layers, which means that the number of layers increases with distance to the object. Based on transmission and reflection more layers result in a higher number of light beams. A reflected light beam which is received by the sensor could have traveled several possible light paths. Hence, the novel approach considers the multiple reflection of light.

Lidar sensors operate according to the time-of-flight measurement principle. The sensor measures the time, which the emitted light pulses need to travel from sensor to target and back. Each measured signal in the receiver must be reflected at least on one object. This object could either be a raindrop or the target.

Assuming a light beam transmits $z-1$ layers, is reflected at the z-th layer and goes straight back to the sensor, so the received intensity can be described as

$$I_z = I_0 \cdot \tau^{2(z-1)} \cdot \varrho \tag{1}$$

where I_z describes the received intensity and I_0 the transmitted intensity of the light beam. τ represents the transmittance of one single layer, while ϱ represents the reflectance of one single layer. The time of flight for one layer is T. The number of traveled layers κ is $(2z-1)$, which is the sum of exponents of τ and ϱ. The time of flight for all layers, represents the product of κ and T. Equation 1 is only valid for one possible light path. The light beam could also be reflected several times. A time of flight of $7 \cdot T$ results in 5 possible combinations of light paths, which are shown in figure 1. The light beam reaches maximum the fourth layer and is one, three or five times reflected. Regarding transmission, T is the time it takes for the light beam to travel the shortest distance within one layer. Assuming that the rain drops are distributed equally, T is regarding reflection the time to travel to the center of the layer and back again. Hence, the time which the light beam needs to travel trough one layer is independent of transmission or reflection exactly T.

The various combinations of light paths occur with varying frequency. The number of occurrence is represented by p. For a known number of transmissions and reflections p can be calculated. Based on this, the sum of received intensities can be described by

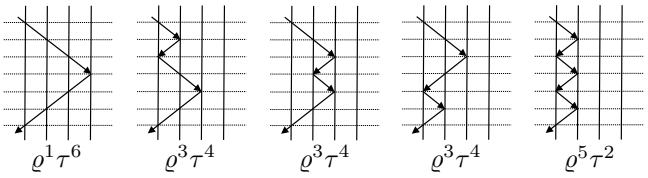

Fig. 1. Possible combination of light paths for $\kappa = 7$

$$I_\kappa = I_0 \cdot \sum_{i=1}^{\frac{\kappa-1}{2}} p_i \cdot \varrho^{2i-1} \cdot \tau^{\kappa+1-2i} \tag{2}$$

where the number of transmissions is expressed by $t = \kappa + 1 - 2i$ and the number of reflections by $r = 2i - 1$. The sum of t and r is κ. If the exponent of τ is decremented by 2, the exponent of ϱ is increased by 2. I_κ is the received intensity, so the light beam must always travel back to the receiver. The number of occurrence p_i can be determined based on Dyck paths.

A Dyck path with the length $2n$ is a diagonal lattice path, which begins at the origin and ends at $(2n; 0)$, consisting of n up-steps (rises) and n down-steps (falls), such that the path never goes below the x-axis. By encoding each rise by the letter U and each fall by the letter D, the so-called Dyck word can be formed [11]. Figure 2 shows an example for the Dyck path and Dyck word of length 6 ($n = 3$), where five different paths of length $2n$ are illustrated.

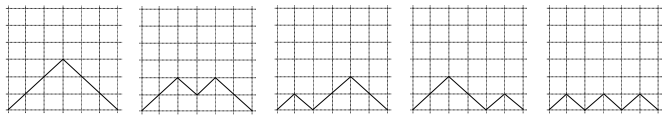

Fig. 2. Dyck path and Dyck word of length 6

The number of paths, which can be determined by the Catalan numbers, can be calculated as follows [11].

$$C_n = \frac{1}{n+1}\binom{2n}{n} \tag{3}$$

The Indian mathematician Narayana (1930-1987) developed the so-called Narayana number, an expression that represents the number of Dyck paths of length $2n$ and k peaks [12].

$$N(n,k) = \frac{1}{n}\binom{n}{k}\binom{n}{k-1} \tag{4}$$

The mathematical problem of Dyck paths can also be used to determine the factor p_i. To calculate the number of combinations, the parameters n and k have to be determined. By using the number of transmissions and reflections, the half path length can be calculated by $n = \frac{\kappa-1}{2}$. The number of peaks k can be calculated by $k = \frac{r+1}{2}$. In the layer model each change of direction is a reflection. Hence, the number

of reflections does not correspond to the number of peaks. It follows

$$n = \frac{\kappa - 1}{2} \tag{5}$$

$$k = \frac{2i - 1 + 1}{2} = i. \tag{6}$$

The two expressions can be used in equation 4 for the Narayana-number that is now called p.

$$p_i = \frac{1}{\frac{\kappa-1}{2}} \cdot \binom{\frac{\kappa-1}{2}}{i} \binom{\frac{\kappa-1}{2}}{i-1} \tag{7}$$

$$= \frac{2}{\kappa - 1} \cdot \binom{\frac{\kappa-1}{2}}{i} \binom{\frac{\kappa-1}{2}}{i-1} \tag{8}$$

Next, the transmission, reflection and absorption of a layer containing raindrops will be determined. The disturbing effects only affect a part β of the light cross section. A significant part of the light passes through the layer unhindered.

To calculate the degree of coverage, the surfaces of all raindrops in one layer are considered. It is assumed that there no overlapping raindrops exist. The water-covered area A_{rain} is the area which is covered with water and can be calculated by the following equation.

$$A_{rain} = d \cdot \int_0^\infty N(D) \cdot \left(\frac{D}{2}\right)^2 \cdot \pi \, dD \tag{9}$$

where d is the thickness of one layer, D is the drop diameter and $N(D)dD$ the concentration of drops having diameters between $D + dD$. The most common used mathematical model to represent the drop size distribution is the exponential distribution by Marshall and Palmer [13]. Now it is recognized that the drop size distribution of natural rain is better represented by the gamma distribution [14]. It is assumed that the proportion of water-covered area of the laser cross-section is equal to the proportion of water-covered area of one square meter. This results in a coverage of:

$$\beta = \frac{A_{rain}}{A_{norm}} \tag{10}$$

where A_{norm} is 1 m^2. This coverage takes an influence on the calculation of the physical effects.

$$\tau = 1 - \varrho - \delta \tag{11}$$

$$\varrho = \beta \cdot \varrho_{rain} \tag{12}$$

$$\delta = \beta \cdot \delta_{rain} \tag{13}$$

τ is transmittance and ϱ the reflectance of a single layer as described before. δ is the absorption of one layer, which describes the energy loss. Reflection occurs when light enters into an optically denser or less dense medium. For this purpose the Fresnel equations can be used to calculate ϱ_{rain} [15]. For this case the Fresnel equations describe what fraction of the light is reflected and what fraction is transmitted. The absorption δ_{rain}, when passing through the water layer can be calculated according to Beer's law [16]. It relates the attenuation of light to the properties of the material through which

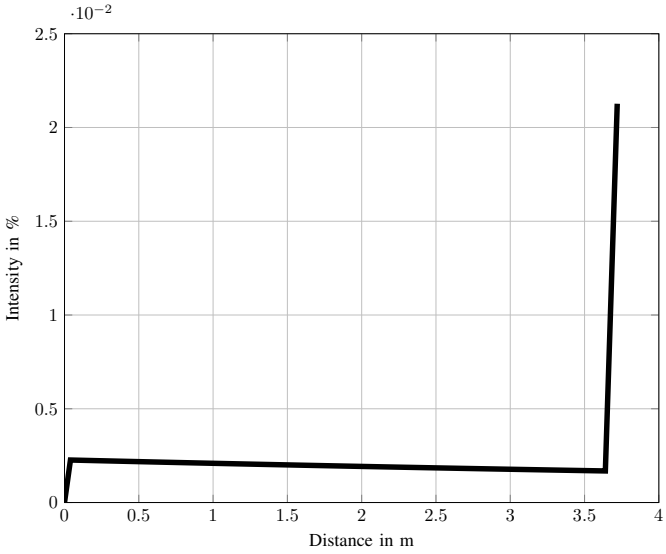

Fig. 3. Graphical illustration of the model

the light is traveling. After the laser beam has passed through all rain layers it hits the object. The received intensity from the object I_{obj} can be described by the following equation.

$$I_{obj} = I_0 \cdot \varrho_{obj} \cdot \tau^{2\kappa} \tag{14}$$

where ϱ_{obj} is the reflectivity of the object. Equation 14 describes the behavior for direct way to the object and back without reflections on layers. The multiple reflection after interaction with the object is not discussed in detail. In this work only the first and largest amplitude is considered.

Figure 3 illustrates the developed model, which is mathematically described by equation 2. The intensity of the received light beam is plotted depending on the traveled distance, which can be determined by the defined layer thickness. It can be seen that the intensity decreases with increasing distance. This effect is based on the increasing number of layers (disturbances). When the light beam hits an object after traveling through rain, a significant increase of intensity can be seen, since the reflectivity of an object is higher then the reflectivity of raindrops. For modeling in figure 3 an object reflectivity of 4% and a rain intensity of 80mm/h was chosen, which corresponds to heavy rain. For the layer thickness, which depends on the sensor distance resolution, the value of the ibeo LUX sensor [10] was selected. The calculation of the degree of coverage is based on the drop size distribution by Deirmendjian [6], [17]. To calculate the reflection, vertical incidence of the laser beam was adopted. Regarding the absorption the mean droplet size has been selected for the distance where the light beam travels through water per layer. This is necessary for the calculation according to Beer's law [16].

The model described in this section will be validated in section V based on tests with a rain simulator. The next section describes the test methodology for the test of automotive sensor systems, which is based on this presented layer model.

IV. Test Methodology

To validate the model a rain simulator was developed and constructed. Researches with rain simulators are more rapid, efficient, controlled, and adaptable than researches under natural rainfall [18]. It is mandatory that the artificial rainfall has the same characteristics as natural rainfall. The special feature of the simulator is that it was designed mobile, so it can be transported easily. For variable height adjustment telescopic profiles are used. The height can be freely adjusted between 3.6 m and 5.6 m. The watering area is 2.2 m x 4 m. The rain will be realized through the use of full cone nozzles. There are always formed 3 pairs of nozzles which produce fine, medium and larger droplets. Thereby, it is possible to replicate a real droplet spectrum. Natural rainfall consists of drop sizes that range from near zero to about 7 mm in diameter. The median drop diameter is between 1 and 3 mm and tends to increase with rain intensity [19]. Small raindrops need a smaller drop height to reach their terminal velocity than larger raindrops [19]. The terminal velocity of raindrops varies from 0.1 to greater than 9 m/s [20]. Thanks to the full-cone nozzles, raindrops have an initial velocity, whereby the required drop height is reduced. The top of the rain simulator was designed that the distances of the nozzles are adjustable. The water is transported with 3 water pumps upwards. Each pump is responsible for a nozzle size. In addition, the water flow rate of each individual nozzle can be adjusted. Thereby, various rain intensities are achieved. Intensities between 12 mm/h and 120 mm/h are usually of greatest importance [18]. When a rain simulator is used outdoors for sensor tests, it is absolutely necessary to measure the additional disturbances such as wind or temperature. Figure 4 shows the developed and constructed simulator for the test of automotive sensor systems. Two static test methods have been developed to test a surround sensor to disturbances. A differentiation is made between object distance variable and rain intensity variable test. These are based on the introduced layer model, described in section III.

A. Object distance variable

The sensor is mounted in front of or in the watering area of the rain simulator. The object to be measured is attached to the sensor as close as possible. Then the artificial rain is initiated. The rain intensity can be variable set depending on the application. The test is based on the increase in the distance between the sensor and the object. The distance from the object is increased in small steps. Based on the model new layers are added, resulting in a controlled increase of the disturbance. The rain intensity is kept constant over the testing process. In order to make statements about the sensor errors, this test procedure is repeated without rain. A rain simulator is helpful but not absolutely necessary for this methodology. Carrying out these tests outdoor, the current precipitation must be measured and documented over the testing process.

B. Rain intensity variable

The sensor is mounted in front or in the watering area of the rain simulator. The object to be measured is fixed to a defined position. In this test case, the distance between sensor and object is kept constant. The intensity of rain starts with 0 mm/h and is increased in small steps. Based on the model, no new layers are added here. The effects occurring per layer cause higher disturbance, due to the higher occurrence of raindrops. As shown in equation 12 and 13, a higher degree of coverage leads to increased effects. To carry out this test method a rain simulator is necessary to save time, since influence is made to the disturbance. The alternative would be very costly long-term tests, which usually do not exceed the local rainfall limits.

Fig. 4. CARISSMA Rain Simulator

This methodologies enable to get control over the disturbing effects. If the sensor is operated under normal conditions and is faced with disturbances during the test process it follows that the change of the output signal is a consequence of the disturbance. Moreover, this method can be used for sensor benchmark. Based on the test method, in which the distance is increased at a constant rain intensity, the distance may be the assessment criterion. Based on the other test method, the rain intensity is the assessment criterion. A sensor is better then another, when it can generate more reliable measurements through more layers. Or a sensor is better than another, when it can measure more reliable in a higher rain intensity. A rainfall simulator allows to perform such studies without further interference effects.

V. Validation

A. Rain Simulator Validation

For the validation of the rain simulator, a laser precipitation monitor (disdrometer) is used. The disdrometer consists of a laser emitter, a receiver, and a digital signal processing unit. The laser diode and some optics produce a parallel infrared light sheet of 0.75 mm thickness with a detection area of 20 x 228 mm^2. The receiver signal is reduced, when particles fall through this beam. The amplitude of the reduction is related to the size of the particles, and the duration to the fall speed. From known statistics of particle size and velocity, the precipitation type is determined. The sensor can detect drizzle, rain, hail, snow, snow grains and ice pellets. The output of this device includes parameters like SYNOP, METAR codes, precipitation intensity and amount, and full particle size and velocity distribution [21].

The disdrometer outputs the measured particle counts per velocity and diameter class. The method to convert the raw number of particles into a per-diameter-class volumetric drop concentration N (m^{-3} mm^{-1}) is described in [22]. The result can be seen in figure 5. It shows the drop size distribution using all nozzle sizes. The produced rain intensity is 94.5 mm/h which corresponds to very stormy rain.

Compared with the distribution as Ulbrich [23] or Deirmendjan [6] clear similarities can be seen. Most drops are located in the low diameter range between 1 mm and 2 mm. Larger drops are less frequent. But it can also be seen that the number of drops is relatively high. This is due to the use of nozzles. In order to achieve the uniform distribution and for watering the intended area, a minimum pressure is required. That is why the rain simulator produces high rain intensities. The lower limit is in range of 40 mm/h and the upper limit is in range of 110 mm/h. For the first tests the rain simulator has reproduced a realistic drop size distribution.

B. Model Validation

For the validation of the model, measurement data is recorded from an object under the influence of rain. For the measurements the Hokuyo UTM-30LX-EW scanning laser range finder (λ=905 nm) is used, which is rated IP67 according to International Protection Marking [24]. This two-dimensional scanning sensor measures horizontal distances to objects in a range up to 30m and provides a relative intensity value for each measured point. As object to be measured, a white and matte plastic plate is chosen, to prevent further absorption.

Figure 6 shows the results of the distance variable and rain intensity variable test. Pyo et al. used in [25] for measuring the position of everyday objects the Hokuyo URG-30LX and showed that due to the hardware constraint of the laser scanner, the intensity is not reliable when the object is located closer than 0.8 m. They also have demonstrated the intensity curve of different materials based on experiments. The intensity values differ depending on the material. The curve progression is basically identical. From a distance of 0.8 m, the intensity decreases with increasing distance. In figure 6 the same behavior

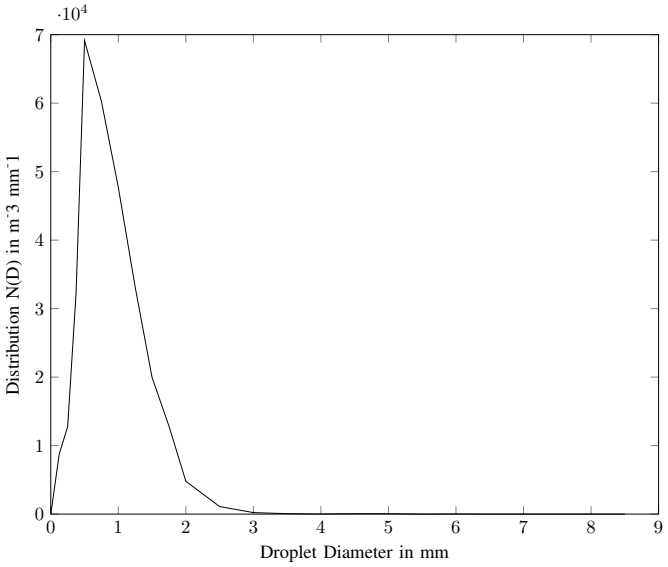

Fig. 5. Drop size distribution of the simulated rain

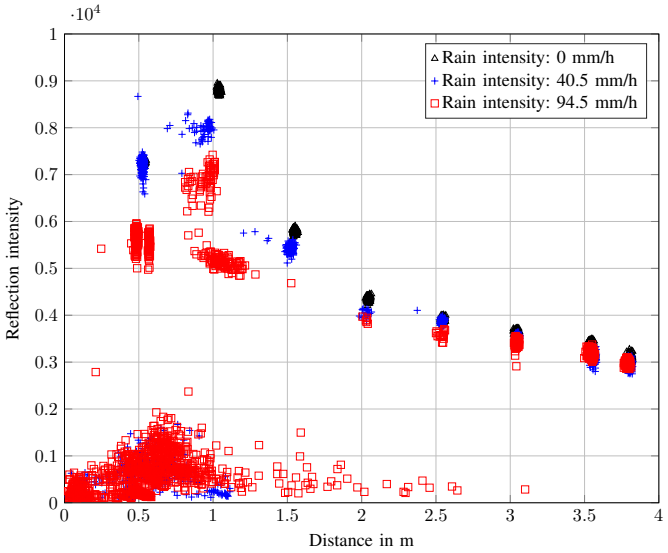

Fig. 6. Measured data of the laser scanner

can be seen. The black triangles represent the intensity values of the object without rain.

The other points have been created in measurements under simulated rain. For the measurement of the blue crosses a rain intensity of 40.5 mm/h was set and for the red squares a rain intensity of 94. 5mm/h. The measurement of the rain intensity is performed by a disdrometer, which is described in the previous subsection.

In figure 3 can be seen the greatest disturbance by rain is near to the sensor. This can also be recognized on the variance of the points from object at 1 m and 1.5 m in figure 6. These differ significantly from the original values (without rain). Looking at the other points it can be seen that the intensity is always less than without rain. This is the case, because water

absorbs the intensity of the emitted laser beam.

If the measured values in the low intensity range are analyzed, the reflection of raindrops can be seen. As well as the developed model shows the intensity values of raindrops are smaller than those from the object. This is due to the higher reflectivity of objects. Because of sensor hardware and laser beam characteristic in case of rain, the intensity of reflected raindrops decreases with increasing distance. The intensity of the object reflection also decreases with increasing distance. Therefore, it is defined as a critical point, when the intensity values of raindrops exceeds the intensity values from the object. This point can not be reached with the current dimensions of the rain simulator.

VI. Conclusion and Future Work

This paper examines the influence of rain on automotive laser scanner sensors. Laser scanners have a huge potential in the field of integrated safety systems. The presented model allows to describe the impact of rain. The distance between sensor and object is divided into layers and the effects per layer are considered in summary. These effects are absorption, transmission and reflection of the light. The transmitted light component passes into the next layer. The reflected light component reverses its direction and enters the previous layer or to the sensor. Based on Dyck path the model also considers multiple reflections of light. By using the Catalan numbers and the Narayana numbers it is ensured that all possible combinations of the light path are covered. Thus statements about the function range of the sensor can be made. The presented test methodologies allow the identification of critical operating points. This is the moment in which the sensor is graded from reliable to unreliable. Safety systems, such as autonomous braking systems, may not make an activation decision based on unreliable sensor data. A false trigger could be fatal for the occupants. A rain simulator has been constructed for the validation of the model. The characteristics of the rain simulator was compared with statistical data from literature and showed a good correlation.

The used laser scanner provides distance and relative intensity values. By processing of absolute raw data values, internal preprocessing can be excluded in the future and the impact of rain will be considered in more detail. Additionally, the theoretical model will be developed further. Effects such as the scattering and the angle of incidence can be taken into account. The water covering on the target object additionally influence the reflection. In the next step it is important to fully validate the rain simulator by using real rain data. The test procedure can be applied to various environmental influences. It can be used for fog, as well as for snow and other weather conditions. It is important that the simulated environment is deterministic. Another part of the future work will be to investigate the influence of the adverse environment on other types of surround sensors e.g. camera or radar sensors. Up to now, only static scenarios have been investigated. Therefore, also dynamic aspects from real driving scenarios have to be considered in future research.

References

[1] R. H. Rasshofer and K. Gresser, "Automotive radar and lidar systems for next generation driver assistance functions," *Advances in Radio Science*, vol. 3, pp. 205–209, 2005.

[2] W. H. Organization, *WHO Global Status Report on Road Safety 2013: Supporting a Decade of Action*. Geneva: World Health Organization, 2013.

[3] B. R. Chang, H. F. Tsai, and C.-P. Young, "Intelligent data fusion system for predicting vehicle collision warning using vision/gps sensing," *Expert Systems with Applications*, vol. 37, no. 3, pp. 2439–2450, 2010.

[4] Jean Andrey and Sam Yagar, "A temporal analysis of rain-related crash risk," *Accident Analysis & Prevention*, vol. 25, no. 4, pp. 465–472, 1993. [Online]. Available: http://www.sciencedirect.com/science/article/pii/0001457593900769

[5] R. H. Rasshofer, M. Spies, and H. Spies, "Influences of weather phenomena on automotive laser radar systems," *Advances in Radio Science*, vol. 9, pp. 49–60, 2011. [Online]. Available: http://www.adv-radio-sci.net/9/49/2011/

[6] D. Deirmendjian, "Electromagnetic scattering on spherical polydispersions," 1969.

[7] J. Wojtanowski, M. Zygmunt, M. Kaszczuk, Z. Mierczyk, and M. Muzal, "Comparison of 905 nm and 1550 nm semiconductor laser ragefinders' performance deterioration due to adverse environmental conditions," 2014.

[8] Koskinen, S., Peussa, P. ed., "Friction project final report," *Deliverable 13 for the European Commission*, 2009.

[9] J.B. Ries, M. Seeger, T. Iserloh, S. Wistorf, and W. Fister, "Calibration of simulated rainfall characteristics for the study of soil erosion on agricultural land," *Soil and Tillage Research*, vol. 106, no. 1, pp. 109–116, 2009. [Online]. Available: http://www.sciencedirect.com/science/article/pii/S0167198709001391

[10] Ibeo Automotive Systems GmbH, *Ibeo LUX Operationg Manual*, 2010.

[11] Emeric Deutsch, "Dyck path enumeration," *Discrete Mathematics*, vol. 204, no. 1–3, pp. 167–202, 1999. [Online]. Available: http://www.sciencedirect.com/science/article/pii/S0012365X98003719

[12] T. V. Narayana, *Lattice Path Combinatorics, with Statistical Applications*, ser. Mathematical Expositions. University of Toronto Press, 1979.

[13] J. S. Marshall, "The distribution of raindrops with size," *The journal of meteorology*, vol. 5 (1948), pp. 165–166, 1948.

[14] Jacques Testud and Stephane Oury, "The concept of normalized distribution to describe raindrops spectra: A tool for cloud physics and cloud remote sensing," 2000.

[15] M. Bass and V. N. Mahajan, *Handbook of optics*, 3rd ed. New York: McGraw-Hill, 2010.

[16] H. Weichel, *Laser beam propagation in the atmosphere*, ser. Tutorial texts in optical engineering. Bellingham, Wash., USA: SPIE Optical Engineering Press, 1990, vol. v. TT 3.

[17] Isaac I. Kim, Bruce McArthur, and Eric J. Korevaar, "Comparison of laser beam propagation at 785 nm and 1550 nm in fog and haze for optical wireless communications," *SPIE Proceedings Vol. 4214*, 2001.

[18] L. D. Meyer, "Simulation of rainfall for soil erosion research," *Transactions of the ASAE 8(63): 63-65*, vol. 1965.

[19] J. O. Laws and D. A. Parsons, "The relation of raindrop-size to intensity," *Transactions, American Geophysical Union*, vol. 24, no. 2, p. 452, 1943.

[20] R. Uijlenhoet and D. Sempere Torres, "Measurement and parameterization of rainfall microstructure," *Journal of Hydrology*, vol. 328, no. 1-2, pp. 1–7, 2006.

[21] Hannelore I. Bloemink, Eckhard Lanzinger, "Precipitation type from the thies disdrometer," *WMO Technical Conference on Instruments and Methods of Observation (TECO-2005), Bucharest, Romania*, pp. 4–7, 2005.

[22] T. H. Raupach and A. Berne, "Correction of raindrop size distributions measured by parsivel disdrometers, using a two-dimensional video disdrometer as a reference," *Atmospheric Measurement Techniques*, vol. 8, no. 1, pp. 343–365, 2015.

[23] Carlton W. Ulbrich, "Natural variations in the analytical form of the raindrop size distribution," *J. Climate Appl. Meteor., 22*, 1983.

[24] Hokuyo Automatic Co.,LTD., "Scanning laser range finder utm-30lx-ew specification," 2012.

[25] Y. Pyo, T. Hasegawa, T. Tsuji, R. Kurazume, and K. Morooka, "Floor sensing system using laser reflectivity for localizing everyday objects and robot," *Sensors (Basel, Switzerland)*, vol. 14, no. 4, pp. 7524–7540, 2014.